

## Particle-core coupling in $^{101-105}\text{Pd}$ : The rotational model at intermediate deformation\*

Hastings A. Smith, Jr.

*Indiana University Cyclotron Facility and Physics Department, Bloomington, Indiana 47401*

F. A. Rickey

*Department of Physics, Purdue University, West Lafayette, Indiana 47907*

(Received 17 May 1976)

Recent (HI,  $xn\gamma$ ) results on the levels of  $^{101,103,105}\text{Pd}$  have been analyzed using the Nilsson model with Coriolis coupling at intermediate deformation ( $\delta \approx 0.12$ ). A variable moment of inertia treatment of the Nilsson basis was found to be necessary. With such a treatment the decoupled  $11/2^-$  and  $7/2^+$  bands of "favored states" are well reproduced for all three nuclei. In addition, the decoupled ( $\Delta I = 2$ ) character of the  $5/2^+$  ground-state band in  $^{101}\text{Pd}$  is explained, as well as its transition to a conventional  $\Delta I = 1$  band in  $^{105}\text{Pd}$ . Some of the other, "unfavored" states in these nuclei are also explained; and single-nucleon transfer spectroscopic factors and relative  $\gamma$ -ray branching are also discussed.

[ NUCLEAR STRUCTURE  $^{101,103,105}\text{Pd}$ ; calculated energy levels ( $d, p$ ) ( $d, t$ ) spectroscopic factors,  $\gamma$ -ray branching. Nilsson model, Coriolis coupling, variable moment of inertia. ]

### I. INTRODUCTION

Studies utilizing (heavy ion,  $xn$ ) reactions have produced bands of states in odd- $A$  Pd<sup>1</sup> and odd- $A$  La<sup>2</sup> nuclei which appear to result from the coupling of an odd particle to the collective motion of an even-even core. The energies of the states in the odd- $A$  bands look as if the ground state band of the even-even core had simply been superimposed on the odd-mass bandhead state without major changes in the configuration of the particle or core states. In this situation, the particle is effectively "decoupled" from (i.e., minimally coupled to) the core and becomes essentially a "spectator" to the motion of the core. Specifically, in the La nuclei, these bands have negative parity and exhibit a  $\Delta I = 2$  spin sequence:  $\frac{11}{2}^-$ ,  $\frac{15}{2}^-$ ,  $\frac{19}{2}^-$ , etc. The experimental results are quite consistent with an extreme weak coupling description of the nuclei, but such an interpretation is independent of any specific description of the collective motion of the core, so it sheds little light on the nuclear structure. An interesting and potentially much more useful interpretation of the odd- $A$  La band structure has been offered by Stephens and co-workers, who have proposed<sup>2</sup> a rotational description of these nuclei. In this description the even-even core is moderately deformed ( $\delta \approx 0.1$  to  $0.2$ ), and Coriolis effects are therefore comparable in energy to the single-particle level spacings. Because of these Coriolis effects the minimum energy is obtained when the angular momentum of the odd particle  $\vec{j}$  and the rotational angular momentum of the even-even core  $\vec{R}$  are maximally aligned. The odd particle's own angular momentum ( $j$ ), being

aligned with that of the core ( $R$ ), gives the odd- $A$  spin sequence  $I = j + R = j, j + 2, j + 4$ , etc. This behavior should be most pronounced for odd-particle states of relatively high single-particle purity and large  $j$ . The unique-parity orbitals ( $g_{9/2}, h_{11/2}, i_{13/2}$ , etc.), which are depressed into the next lower major oscillator shells by the spin-orbit interaction, are therefore most likely to exhibit this "decoupled" behavior. The observed band structure of the odd- $A$  La nuclei can then be interpreted as arising from the Coriolis coupling of an odd  $h_{11/2}$  proton to the motion of the adjacent even-even Ba core. The correct energy spacing and angular momentum sequence for the odd- $A$  bands are then predicted because of the specific nature of the particle-core coupling and *not* because the coupling is weak.

Similar negative-parity band structure has also been observed<sup>1</sup> in the odd- $A$  Pd nuclei,  $^{101-105}\text{Pd}$ . In addition, definite  $\Delta I = 2$  *positive*-parity bands, built on  $I = \frac{7}{2}$  and  $I = \frac{5}{2}$  states, have been seen in these nuclei. In analogy with the odd- $A$  La nuclei, the Pd negative-parity band structure could be interpreted as the Coriolis decoupling of an odd  $h_{11/2}$  neutron from the adjacent even-even Pd core. In addition, it is tempting to attribute the positive-parity band structure to the partial decoupling of  $g_{7/2}$  and  $d_{5/2}$  odd neutrons. In this latter case, one would expect that the highest- $j$  positive-parity orbital, namely  $g_{7/2}$ , would exhibit the most significant decoupling behavior, with the next highest  $j, d_{5/2}$ , decoupling to a lesser extent. In fact, the experimental data show that the  $\frac{7}{2}^+$   $\Delta I = 2$  band persists in all three nuclei studied. On the other hand, the  $\frac{5}{2}^+$   $\Delta I = 2$  band is definitely present<sup>3</sup> only

in  $^{101}\text{Pd}$ ; it is weakly seen<sup>4</sup> in  $^{103}\text{Pd}$  and absent in  $^{105}\text{Pd}$ . In fact, in  $^{105}\text{Pd}$  it is replaced by a  $\frac{5}{2}^+$   $\Delta I=1$  band.<sup>5</sup>

It should be further noted that in  $^{103}\text{Pd}$  and  $^{105}\text{Pd}$  a number of states other than those associated with the  $\frac{11}{2}^-$ ,  $\frac{5}{2}^+$ , and  $\frac{7}{2}^+$  bands have been observed.<sup>4,5</sup> These states actually constitute an added constraint on the model used to describe nuclei in this region, and their role in the test of the present calculation will be discussed in the ensuing sections.

In this paper we shall demonstrate that the negative parity  $\Delta I=2$  band built on an  $\frac{11}{2}^-$  state in  $^{101-105}\text{Pd}$  can be understood as a Coriolis-decoupled band with a dominant  $K$  value of  $\frac{1}{2}$ , indicating a maximum alignment of  $\vec{j}$  and  $\vec{R}$ . We will also present the results of a Nilsson model calculation with Coriolis coupling on the positive-parity states in these nuclei, in an effort to demonstrate that the rotation alignment and consequent decoupling is capable of explaining these states as well. Finally, we shall show that this rotational model also provides a natural explanation of the other negative- and positive-parity states seen in  $^{103,105}\text{Pd}$ .

## II. DESCRIPTION OF CALCULATION

The calculation employs a modified version of a computer code originally written by Starner and Bunker<sup>6</sup> which utilizes the standard Nilsson model<sup>7</sup> for an odd particle coupled to an axially symmetric deformed core. The total Hamiltonian is taken as  $H=H(\text{Nilss})+H(\text{rot})$ , where  $H(\text{Nilss})$  is the usual single-particle deformed shell model Hamiltonian<sup>7</sup> with energy eigenvalues  $e_K$ , and  $H(\text{rot})$  constitutes the energy of the system which comes from collective rotation and includes the recoil and Coriolis terms (see below). Specifically,

$$\begin{aligned} H(\text{rot}) &= \frac{1}{2g} [\vec{I} - \vec{j}]^2 \\ &= \frac{1}{2g} [I^2 + j^2 - 2I_3 j_3 - (I_+ j_- + I_- j_+)]. \end{aligned} \quad (1)$$

The last term is the so-called Coriolis term, and the components of  $\vec{j}$  and  $\vec{I}$  are with respect to the nuclear body-fixed axes, the 3 axis being the symmetry axis.

A Nilsson diagram appropriate for odd-neutron nuclei in this mass region is shown in Fig. 1. The shell model parameters  $\kappa$  and  $\mu$  were adjusted so that the  $d_{5/2}$ ,  $g_{7/2}$ ,  $s_{1/2}$ , and  $d_{3/2}$  level positions at zero deformation corresponded to those determined by Reehal and Sorensen.<sup>8</sup> The values of  $\kappa$  and  $\mu$  thus obtained were 0.064 and 0.35, respectively, which also correspond to the values suggested by Soloviev.<sup>9</sup> The  $h_{11/2}$  basis states were calculated using  $\kappa=0.066$  and  $\mu=0.35$  and were

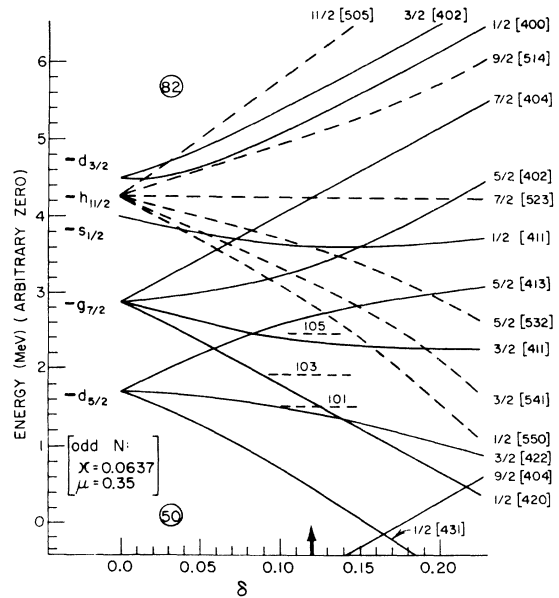


FIG. 1. Nilsson diagram for odd neutrons in the  $A=103$  mass region. The positions of the spherical shell model states in this region (see Ref. 8) are shown as heavy lines to the left of the diagram, and the shell-model parameters  $\kappa$  and  $\mu$  were adjusted to values of 0.0637 and 0.35 to obtain correspondence between these levels and the Nilsson levels at zero deformation. Fermi levels chosen for the  $A=101, 103, 105$  isotopes of Pd are indicated by the dashed horizontal lines, and the energy scale is based on  $\hbar\omega_0 = 41/A^{1/3}$  MeV for  $A=103$ .

placed at an energy relative to the above-mentioned positive-parity shell model states which was consistent with the results of Reehal and Sorensen.<sup>8</sup>

The level structure of the even-even Pd nuclei, if interpreted in a quasirotational context, suggests an intermediate deformation of  $\delta=0.1$  to  $0.2$  for the low-lying states of these nuclei. Measurements of  $B(E2, 0^+ \rightarrow 2^+)$  in the even-even Pd nuclei<sup>10</sup> suggest  $\delta=0.12$  for  $^{104}\text{Pd}$ . Furthermore, the  $B(E2, 0^+ \rightarrow 2^+)$  are decreasing with decreasing mass in this region, so the deformations of  $^{101-105}\text{Pd}$  should remain low. We have therefore used the deformation parameter  $\delta=0.12$  for all of our calculations.

The single-particle energies  $e_K$  of the Nilsson states at this deformation were transformed into quasiparticle energies  $E_K$  according to

$$E_K = [(e_K - \lambda)^2 + \Delta^2]^{1/2} - \Delta, \quad (2)$$

where  $\lambda$  is the Fermi level and  $\Delta$  is the pairing gap parameter. The latter was chosen to be 1.1 MeV for all three Pd nuclei, as suggested by the empirical relation  $\Delta \approx 12/A^{1/2}$  MeV,<sup>11</sup> and also as deduced from the odd-even Pd mass differences in this region. The Fermi levels chosen for each nucleus are also indicated in Fig. 1. The six

unique-parity adiabatic Nilsson states from the  $h_{11/2}$  spherical shell model orbital and the rotational excitations built upon them served as the basis for the calculation of the negative-parity states. The  $N=4$  positive-parity states (excluding the five  $g_{9/2}$  states which are deep in the  $N=3$  oscillator shell) and their rotational excitations were used as the basis for the Coriolis calculation of the positive-parity levels. This basis will be denoted by  $|IMK\rangle$ .

The calculation of the unperturbed bandhead energies also incorporated an approximation to the "zero-point" rotational energy.<sup>12,13</sup> The energies of the states in a Nilsson rotational band are written as

$$E_{IK} = E_K + \frac{1}{2\mathcal{I}} [I(I+1) - 2K^2 + \langle j^2 \rangle] + \delta_{K1/2} a (-1)^{I+1/2} (I + \frac{1}{2}), \quad (3)$$

where the  $E_K$  are the intrinsic *quasiparticle* state energies defined in Eq. (2), and  $a$  is the decoupling parameter for  $K = \frac{1}{2}$  bands ( $\hbar = 1$ ). The quantity  $\langle j^2 \rangle$ , which contributes significantly to this zero-point energy for high- $j$  low- $K$  orbitals, was taken as

$$\langle j^2 \rangle \approx \sum_j C_{jK}^2 j(j+1), \quad (4)$$

where the  $C_{jK}$  are the expansion coefficients of the Nilsson state of the odd particle in the spherical basis. The unperturbed bandhead energies are then given by  $E(\text{bandhead}) = E_{KK}$ .

The Nilsson Hamiltonian was supplemented by the usual Coriolis interaction  $H_{K,K'}$  whose matrix elements in the  $|IMK\rangle$  basis are

$$H_{K,K'} = (U_K U_{K'} + V_K V_{K'}) \langle IMK | H_{\text{Cor}} | IMK' \rangle, \quad (5)$$

where  $\langle IMK | H_{\text{Cor}} | IMK' \rangle$  are the *single-particle* Coriolis matrix elements in the adiabatic basis, and the factor  $U_K U_{K'} + V_K V_{K'}$  is the usual pairing correction factor for the Coriolis matrix elements in a quasiparticle basis. Blocking effects were ignored in the calculation, resulting in a constant  $\lambda$  and  $\Delta$  for all of the intrinsic states of each nucleus.

The total Hamiltonian (including the Coriolis term) was diagonalized, giving the energy eigenvalues and wave functions of the final states  $|IM\rangle$  in terms of the Coriolis mixing amplitudes  $f_{IK}$  and the basis states  $|IMK\rangle$ :

$$|IM\rangle = \sum_K f_{IK} |IMK\rangle. \quad (6)$$

In order to identify the rotational composition of the final states  $|IM\rangle$ , we expand those states in terms of states with good  $R$  and  $j$ , where  $R$  is the

angular momentum of the core,  $j$  is the angular momentum of the odd particle, and  $\vec{I} = \vec{R} + \vec{j}$ . One finds that<sup>14</sup>

$$|IM\rangle = \sum_{jR} \sum_K f_{IK} \alpha_{jR}^{(K)} |IMjR\rangle, \quad (7)$$

where

$$\alpha_{jR}^{(K)} = \sqrt{2} \langle IKj - K | R0 \rangle (-1)^{j-K} C_{jK}. \quad (8)$$

The fraction of the state  $|IM\rangle$  which contains  $R = R_0$  is then given by

$$P(IM, R_0) = \sum_j \langle IMjR_0 | IM \rangle^2 = \sum_j \left( \sum_K f_{IK} \alpha_{jR_0}^{(K)} \right)^2. \quad (9)$$

The single-nucleon-transfer spectroscopic factors for stripping and pickup reactions can be calculated and also serve as a very useful test of the validity of the model used. These factors  $S_I$  are defined by

$$\frac{d\sigma}{d\Omega}(d, t) = N S_I \frac{d\sigma}{d\Omega} \Big|_{\text{DW}}, \quad (10)$$

$$\frac{d\sigma}{d\Omega}(d, p) = N' (2I+1) S_I \frac{d\sigma}{d\Omega} \Big|_{\text{DW}},$$

where  $N$  and  $N'$  are calculated normalization factors for the reaction, and  $(d\sigma/d\Omega)_{\text{DW}}$  are the  $l$ -dependent DWBA differential cross sections. In terms of the Coriolis-perturbed Nilsson wave function, these spectroscopic factors are given by

$$S_I(d, t) = 2 \left( \sum_K f_{IK} C_{IK} V_{IK} \right)^2, \quad (11)$$

$$(2I+1) S_I(d, p) = 2 \left( \sum_K f_{IK} C_{IK} U_{IK} \right)^2,$$

where the quantities  $U_{IK}$  and  $V_{IK}$  refer to the *target* nucleus.

It should be noted that the states of the Pd cores in these odd- $A$  calculations clearly do not exhibit the well-behaved rotational structure that one encounters in the rare-earth region (see, e.g., Ref. 15). An  $I(I+1)$  energy dependence for the members of the ground-state rotational bands, fitted to the first  $2^+$  state, progressively overestimates the energies of the rest of the rotational states. It is possible to impose some compression in energy of the higher-spin members of a rotational band if the energies of the rotational states in the *input* to the odd- $A$  calculation are defined by

$$E_{IK} = E_{KK} + A I(I+1) + B I^2(I+1)^2, \quad (12)$$

where  $A$  denotes the moment of inertia parameter  $1/2\mathcal{I}$  ( $\hbar = 1$ ). However, while this procedure yields results which are in better agreement with experi-

ment than a simple stiff-rotor picture (without the parameter  $B$ ), those results still show a marked progressive overestimation of the energies of the rotational states. This implies that a constant moment of inertia picture for these nuclei is unrealistic, even with the (modest) higher-order corrections provided by the parameter  $B$ .

Viewed in a quasirotational context, the moments of inertia of even-even Pd core states are, in fact, a strong function of the angular momentum. To illustrate this we present in Fig. 2 a plot of the effective moment of inertia parameters for the ground-state quasirotational bands in the even-even Pd cores. This effective moment of inertia parameter  $A(R)$  is defined below for values of the core rotational angular momentum  $R$ :

$$A(R) = \frac{1}{2\mathcal{G}_R} \equiv \frac{E_R - E_{R-2}}{2(2R-1)}. \quad (13)$$

Thus,  $A(R)$  is a spin-dependent (variable) moment of inertia parameter analogous to  $A$  in Eq. (12), with  $B=0$ .

The specification of the input basis states for the

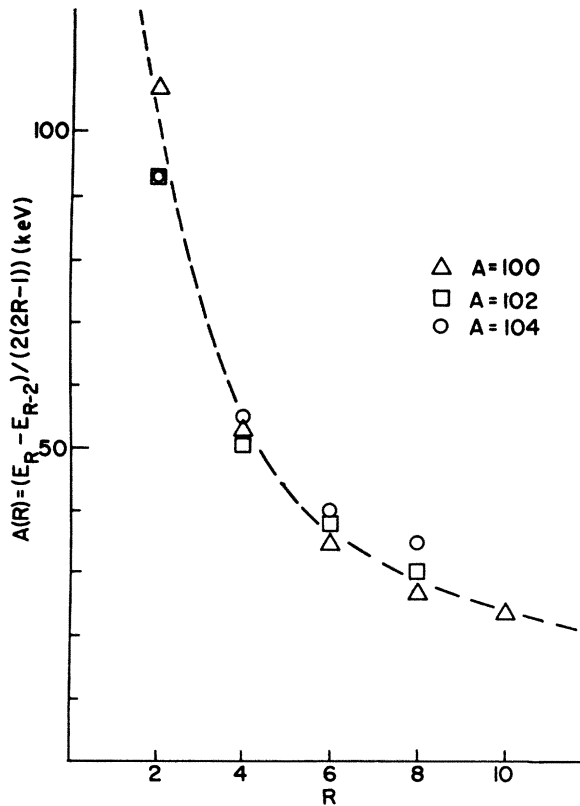


FIG. 2. Empirical moment of inertia parameters  $A(R)$  for the even-even Pd nuclei  $A=100-104$ . [See Eq. (13).] The dashed curve through the data is meant only as a guide to the eye.

odd- $A$  calculation should reflect the “rotational content” of each state, as far as the varying effective moment of inertia parameter is concerned. One way to accomplish this involves assuming that the rotational behavior of each odd- $A$  Pd nucleus is dominated by that of the adjacent even-mass Pd core. Then each unperturbed rotational state in a given Nilsson band  $\{|IMK\rangle\}$  could be characterized by the fraction of each value of the core angular momentum  $R$  allowed by the vector coupling of  $\vec{R}$  and  $\vec{j}$  to  $\vec{I}$  contained in that state. These fractions are given by a special case of Eq. (9) with no Coriolis mixing:

$$P(IKR) = \sum_j (\alpha_{jR}^{(K)})^2. \quad (14)$$

The effective moment of inertia parameter for each rotational state  $|IK\rangle$  can then be expressed as  $1/(2\mathcal{G}_{IK})$ , where  $\mathcal{G}_{IK}$  is the weighted sum of the core moments of inertia for each value of  $R$  contained in that state, the weighting factors being  $P(IKR)$ . Thus,

$$\mathcal{G}_{IK} \equiv \sum_R \mathcal{G}_R P(IKR), \quad (15)$$

$$A_{IK} = 1/(2\mathcal{G}_{IK}).$$

The energies of the unperturbed rotational states  $|IK\rangle$  would then be

$$E_{IK} = E_K + A_{IK}[I(I+1) - 2K^2 + \langle j^2 \rangle + \delta_{K1/2} a(-1)^{I+1/2}(I+\frac{1}{2})] + \frac{1}{2} C (\mathcal{G}_{IK} - \mathcal{G}_{0K})^2. \quad (16)$$

The last term in Eq. (16) is added in analogy with the variable-moment-of-inertia (VMI) model<sup>16</sup> to provide the expected “elastic energy” term. This elastic energy also implies an added potential term in the total Hamiltonian mentioned at the beginning of this section. The elastic constant  $C$  would be obtained most reasonably from a VMI fit to the even- $A$  Pd core. The minimum moment of inertia  $\mathcal{G}_{0K}$  is best defined as

$$\mathcal{G}_{0K} = \mathcal{G}_{IK}(I=j_0), \quad (17)$$

where  $j_0$  is the angular momentum of the spherical shell model state to which the state  $|IMK\rangle$  degenerates at zero deformation.

Although the above procedure is a straightforward way to simulate approximately the core behavior in odd- $A$  bands, it suffers from an intrinsic lack of self-consistency. The weighting factors  $P(IKR)$ , used to calculate the moments of inertia, depend intimately upon the deformation through the  $C_{jK}$  coefficients in  $\alpha_{jR}^{(K)}$  [see Eqs. (7) and (14)]. Thus, a correct calculation of the moments of inertia in a rotating nucleus whose deformation is

not constant must necessarily include a different set of  $C_{jK}$ 's for each rotational state. The weighting factors  $P(IKR)$  must therefore be redetermined for each rotational state in a manner which generates a self-consistent set of moments of inertia.

As a consequence of the complication inherent in the calculation described above, we have adopted an alternative approach to imposing a relativistic core behavior on the unperturbed odd-particle state. This procedure involves an adaptation of the VMI model<sup>16</sup> for these states. In the even-even Pd cores, VMI fits to the ground-state quasirota-tional bands<sup>15</sup> yield elastic constants,  $C$ , of order of  $6 \times 10^6$  keV<sup>3</sup> and a negligible ground-state moment of inertia  $\mathcal{G}_0$ . The minimization of the rotational energy at each spin  $I$  and with  $\mathcal{G}_0 = 0$  simplifies to

$$\mathcal{G}_{IK} = \mathcal{G}_{I0} = [I(I+1)/2C]^{1/3} \text{ keV}^{-1}. \quad (18)$$

As a first approximation, we therefore express the odd- $A$  moments of inertia as

$$\mathcal{G}_{IK} = \left\{ (1/2C) [I(I+1) - 2K^2 + \langle j^2 \rangle + \delta_{K1/2} a (-1)^{I+1/2} (I + \frac{1}{2})] \right\}^{1/3}. \quad (19)$$

The rotational energies to be used as input to the Coriolis calculation are then expressed as in Eq. (16). In the Coriolis calculation  $C$  and  $\mathcal{G}_{0K}$  were treated as free parameters, to be varied over restricted ranges. In addition, the moment of inertia parameter which appears as the energy scale factor in the Coriolis matrix element  $H_{KK'}$ , was set equal to the average value of  $A_{IK}$  and  $A_{IK'}$ .

Plots of the effective moment of inertia parameters [determined from Eq. (19) with  $C = 4 \times 10^7$  and  $3 \times 10^7$  keV<sup>3</sup> for the negative- and positive-parity bands, respectively] are presented in Figs. 3(a)–3(c). The spin dependence of  $\mathcal{G}_I$  is seen to be monotonic in all bands except the  $K = \frac{1}{2}$  bands, where the presence of the diagonal Coriolis term induces oscillations in  $\mathcal{G}$  with spin. This behavior is not surprising in view of the  $R$  content of the rotational states of these bands, which can be discerned by evaluating Eq. (14) for the  $K = \frac{1}{2}$  bands. In fact, this oscillation is essential to the success of the present calculation; a constant or monotonically increasing  $\mathcal{G}$  in the  $K = \frac{1}{2}$  bands yields energy levels which in no way resemble the observed spectra.

Volkov<sup>17</sup> and also Gregory and Taylor<sup>18</sup> have demonstrated that, when Coriolis effects can be ignored, a direct extension of the VMI model<sup>16</sup> from the even-even cores to their adjacent odd- $A$  partners gives reasonable results for the odd- $A$  band energies. While our simplified procedure differs somewhat from the conventional VMI procedure, the end result for the odd-mass input states is basically the same.

The performance of this Coriolis calculation requires that a substantial number of input parameters, including  $E_{KK}$ , a set of  $A_{IK}$ 's for each Nilsson band [see Eq. (16)],  $\kappa$ , and  $\mu$  be specified. In addition, the intrinsic Coriolis matrix elements (including the decoupling parameter for the  $K = \frac{1}{2}$  bands) must, in general, be adjusted. This latter adjustment is usually necessary in the rare-earth region where Coriolis matrix elements are found to be significantly smaller than their theoretical size,<sup>19</sup> and it would not be unreasonable to expect similar behavior in the Pd nuclei.

In a calculation with so many possible input parameters, it is tempting to adjust all of them individually and obtain a best fit, in the most rigorous sense, to the experimental data. On the other hand, it is the objective of this work to attempt an understanding of the odd- $A$  Pd band structure first on the basis of a *simple* application of the Nilsson model with Coriolis coupling. Accordingly, full-scale variation of the input parameters was held to a minimum, and most of the parameters were held within rather restricted ranges of physically reasonable values. In particular, the strength of the Coriolis coupling among all of the basis states was reduced to 80% of its theoretical value. In accordance with Bunker and Reich,<sup>20</sup> we impose this reduction through  $\eta_{KK'}$ , a multiplier of the Coriolis matrix element  $H_{KK'}$ , of Eq. (5). We also define  $\eta_{KK}$  to be equal to the multiplier of the decoupling parameters for the  $K = \frac{1}{2}$  bands and equal to zero for  $K \neq \frac{1}{2}$ . This adjustment of the Coriolis strengths serves the function of approximating several possible effects: (1) a true rescaling of the strength of the rotation particle coupling, (2) a renormalization of the moment of inertia parameters due to polarization of the core by the odd particle or other changes in the nuclear deformation, (3) the influence of the core overlap integrals, defined by Malik and Scholz,<sup>21</sup> and (4) the inclusion of blocking effects and the consequential change in the pairing reduction factors for  $H_{KK'}$  [see Eq. (5)], the last two effects being related.

### III. RESULTS

#### A. Negative parity states

The present state of knowledge regarding the negative-parity states in <sup>101–105</sup>Pd is summarized in Fig. 4. Each of these nuclei shows a definite  $\Delta I = 2$  band of "favored" states, based on an  $\frac{11}{2}$  state, and the character of this band in all three nuclei is essentially unchanged. Furthermore, we see  $\frac{7}{2}^-$  and  $\frac{3}{2}^-$  states in <sup>105</sup>Pd,<sup>22,23</sup> and the same states are tentatively observed<sup>24,25</sup> in <sup>103</sup>Pd. In addition, a few higher-spin negative-parity states

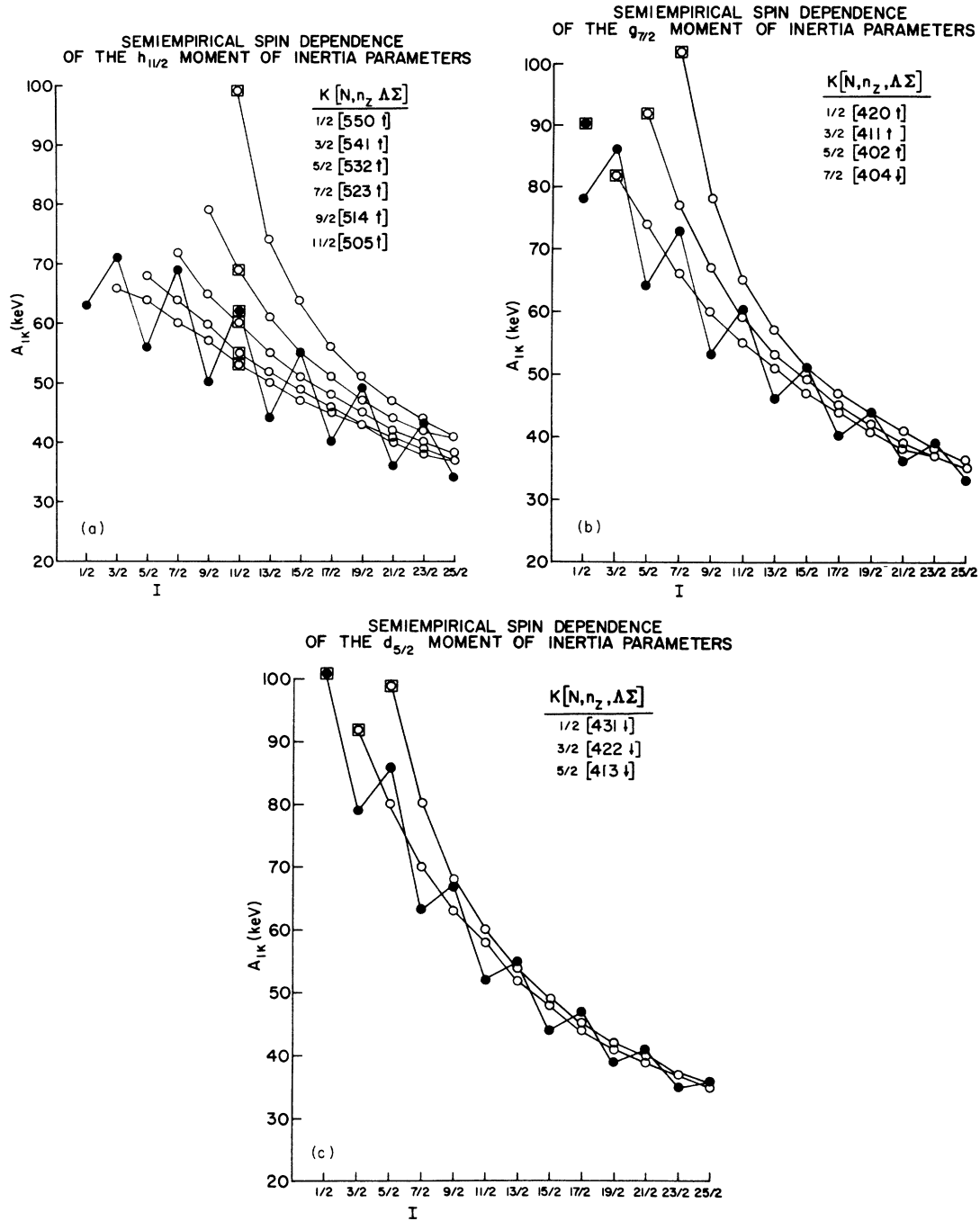


FIG. 3. Semiempirical moment of inertia parameters for the odd-neutron Nilsson states whose parentage is the  $h_{11/2}$  spherical shell-model state. These states are listed in the figure according to their asymptotic quantum numbers. Note that the  $A_{IK}$  curve for each  $K^\pi[Nn_z\Lambda]$  state begins at  $I=K$ . The points enclosed in squares represent the value of the parameter  $1/(2d_{0K}^2)$  used for each band. [See Eqs. (16) and (19).] (b) Same as (a), except for  $g_{7/2}$  states (see also Table II). (c) Same as (a) except for  $d_{5/2}$  states (see also Table II).

have been observed<sup>5</sup> in  $^{105}\text{Pd}$ . Thus, the negative-parity states seen in these Pd nuclei provide a stringent test for the rotational description of a nucleus outside the known deformed regions, since

several levels other than the favored  $\frac{11^-}{2}, \frac{15^-}{2}, \dots$  sequence are known in two of these nuclei.

The negative-parity calculations agree quite well with experiment and yield similar results for

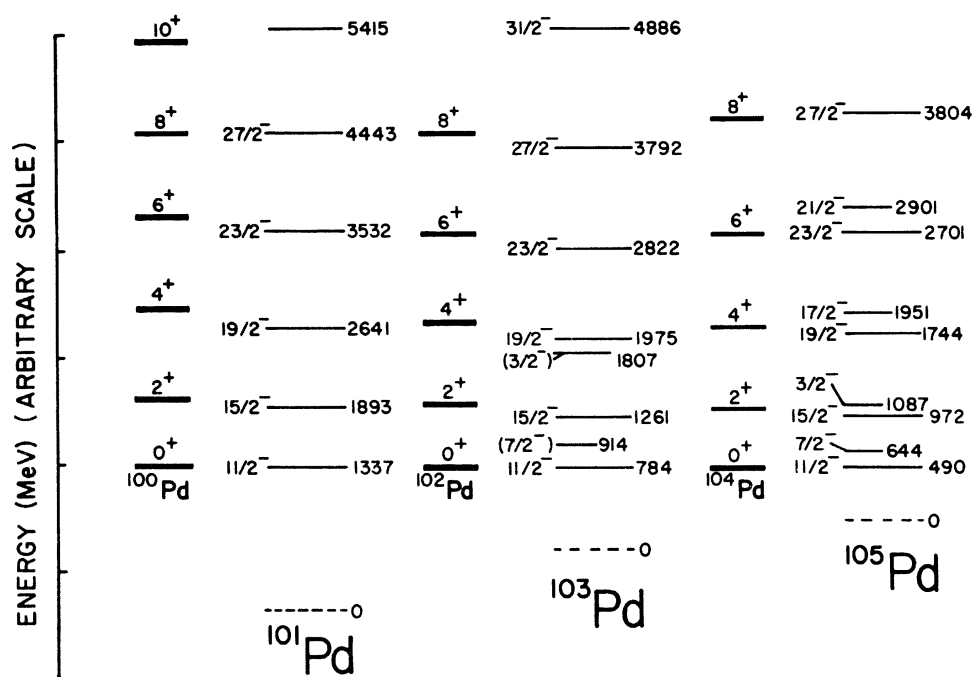


FIG. 4. Summary of experimental knowledge of the negative-parity states in  $^{101}\text{Pd}$  (Ref. 3),  $^{103}\text{Pd}$  (Refs. 4, 24, and 25), and  $^{105}\text{Pd}$  (Refs. 5 and 22). Also shown for comparison are the ground-state (quasirotational) bands of the adjacent even-even Pd cores. The positions of the ground states of the odd-A Pd nuclei are indicated by the dashed horizontal lines.

the negative-parity states in all three odd-A Pd nuclei studied. The only parameters varied in adjusting the calculations for the three nuclei were the Fermi level and mass number; and the final results for the three cases differ basically only in the energy "zero". Subsequent discussion of the negative-parity results will center on  $^{105}\text{Pd}$  levels.

The results for the calculation on  $^{105}\text{Pd}$  are presented in detail in Fig. 5 and discussed below. We have obtained very good agreement with the  $\frac{11}{2}^-$   $\Delta I=2$  band. It is even more important that the same calculation is remarkably accurate in predicting the location of the two low-spin negative parity states and the other, high-spin unfavored states that have been observed experimentally. These latter states are not consistent with the weak coupling picture (where, for instance, the  $\frac{7}{2}^-$  and  $\frac{3}{2}^-$  states would be degenerate with the  $\frac{15}{2}^-$  and  $\frac{19}{2}^-$  states, respectively), and we know of no other adequate interpretation of these states prior to the present calculation.

The angular momentum of states in the  $\frac{11}{2}^-$  band appear to be the result of an alignment of the particle ( $j$ ) and core ( $R$ ) angular momentum ( $I=j+R$ ). As will be shown below, this simplified picture is consistent with the detailed calculation so we will refer to these states as "rotation aligned". The  $\frac{7}{2}^-$  and  $\frac{3}{2}^-$  states are calculated to have dominant  $R=2$  and 4 components, respectively,

so these states are interpreted as "rotation anti-aligned" ( $I=|j-R|$ ).

Since the significance of our calculations is strongly dependent on the proper identification of the  $\frac{11}{2}^-$  band and the  $\frac{7}{2}^-$  and  $\frac{3}{2}^-$  states, a brief review of the appropriate experimental data will be presented. The  $\frac{11}{2}^-$  state in  $^{105}\text{Pd}$  is well established,<sup>28</sup> having been seen in ( $d,p$ ) and ( $d,t$ ) reactions with an  $l$  transfer of 5. Also, its transition probability is in good agreement with that expected for an  $M2$  transition to a  $\frac{7}{2}^+$  state (approximately  $\frac{1}{3}$  of the single-particle value). Delayed coincidence measurements were necessary to assign the states in the  $\frac{11}{2}^-$  band because the  $\frac{11}{2}^-$  state is isomeric ( $\tau_{1/2}=37 \mu\text{sec}$ ). The stretched  $E2$  nature of the  $\gamma$ -ray cascade coming from the band was determined by measuring the  $A_2$  and  $A_4$   $\gamma$ -ray angular distribution coefficients with 1% accuracy. A preliminary report on these measurements for the  $\frac{11}{2}^-$  band has been presented previously<sup>1</sup> and a more complete report<sup>5</sup> is being prepared.

The crucial assignment of the angular momentum and parity of the  $\frac{7}{2}^-$  and  $\frac{3}{2}^-$  states comes from the work of Kawakami and Hisataki,<sup>22</sup> who make very precise measurements of conversion coefficients as well as  $L$ -subshell ratios for transitions following the  $\beta$  decay of the  $\frac{1}{2}^-$  ground state of  $^{105}\text{Ag}$ . The assignments were confirmed by  $\gamma$ - $\gamma$  angular correlation measurements on the same transitions

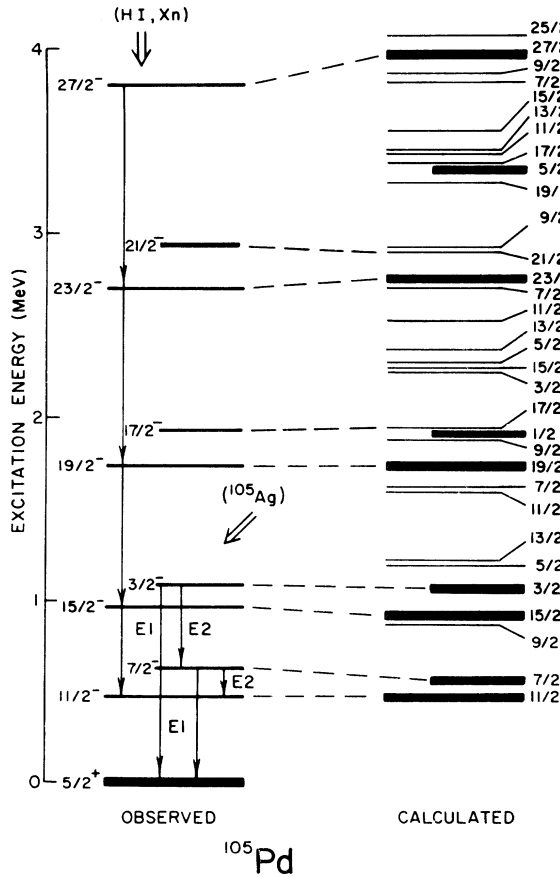


FIG. 5. Detailed summary of the experimental and theoretical results for the negative-parity states in  $^{105}\text{Pd}$ . The heavy lines in the calculated spectrum represent the states which are predicted by the present calculation to comprise the rotation-aligned (longer lines) and rotation-antialigned (shorter lines) bands discussed in the text.

by Behar and Grabowski.<sup>23</sup>

A summary of the most important results of the Coriolis calculation for the negative-parity states in  $^{105}\text{Pd}$  are given in Table I. First, we notice that the states identified as rotation aligned ( $\frac{11}{2}^-$ ,  $\frac{15}{2}^-$ ,  $\frac{19}{2}^-$ , etc.) are all predominantly  $K = \frac{1}{2}$  (i.e., the projection of  $j$  on the nuclear symmetry axis is minimum, so  $j$  and  $R$  are maximally aligned). Rotation alignment is also evident in the dominant  $R$  component—the bandhead is calculated to be primarily  $R=0$ , the first rotational state  $R=2$ , etc. Since the dominant components of the rotation-aligned states come from the same Nilsson band ( $K = \frac{1}{2}$ ), transitions between these states are “intra-band,” so they are expected to have  $B(E2)$ 's that are enhanced, and our calculation predicts an enhancement of about a factor of 30 to 40 times single particle estimates. This is consistent with experimental observation.<sup>1,5</sup>

The identification of the antialigned ( $\frac{11}{2}^-$ ,  $\frac{7}{2}^-$ ,  $\frac{3}{2}^-$ ,

$\frac{1}{2}^-$ , and  $\frac{5}{2}^-$ ) band is also evident from Table I. Again the states are predominantly  $K = \frac{1}{2}$  and have the expected major  $R$  components, except in this case  $I = |j - R|$ . The calculation predicts an even greater  $B(E2)$  enhancement for the antialigned band—typically 45 single-particle units. Since the antialigned states have low angular momentum relative to the aligned states, they are observed to decay by  $E1$  transitions to states outside the bands, so that a more quantitative comparison can be made to the predictions of the Coriolis calculation. The ratios of the  $E2$  (intra-band) to  $E1$  (extra-band) transition probabilities shown in Fig. 5 are observed<sup>22</sup> to be  $4.3 \times 10^{-2}$  and  $2.9$  for the  $\frac{7}{2}^-$  and  $\frac{3}{2}^-$  states, respectively. Even if the  $E1$  transitions were hindered by a factor of  $10^4$ , the single-particle estimates for these ratios would be  $2 \times 10^{-5}$  and  $5 \times 10^{-3}$ , respectively. Thus, both  $E2$  transitions would appear to be enhanced by approximately three orders of magnitude relative to this estimate for the hindrance of the  $E1$  transitions.

Two other high-spin negative-parity states ( $\frac{17}{2}^-$  and  $\frac{21}{2}^-$ ) have been observed in the  $(\text{HI}, xn)$  work.<sup>5</sup> As is evident in Fig. 5 and Table I, the calculation predicts the energies of these states very well.

An important feature of the calculation is that spectroscopic factors for  $(d, p)$  and  $(d, t)$  reactions to final states in  $^{105}\text{Pd}$  can easily be obtained. For a spin-zero target, the stripping spectroscopic factor is given by<sup>27</sup>

$$S_I = \frac{2}{2I+1} \left( \sum_k f_{Ik} C_{Ik} U_{Ik} \right)^2.$$

The calculation predicts that the stripping strength (for negative-parity states) should go predominantly to the  $\frac{11}{2}^-$  states at 490 and 1584 keV:

$$490 \text{ keV: } S_I = \frac{1}{(2I+1)} 6.28,$$

$$1584 \text{ keV: } S_I = \frac{1}{(2I+1)} 2.65.$$

The spectroscopic factor for stripping to the 490 keV  $\frac{11}{2}^-$  state has been measured to be<sup>28</sup>

$$(2I+1)S_I = 6.0 \pm 0.5,$$

in good agreement with the results of the calculation. [No higher-lying  $\frac{11}{2}^-$  states following the  $(d, p)$  reaction were seen, due to the high density of states above 1.5 meV.]

The measured spectroscopic factor cannot be easily explained on the basis of either the simple shell model or a weak coupling model. In either model the splitting of the  $\frac{11}{2}^-$  one-quasiparticle strength is expected to be small. Thus, when only one low-lying  $\frac{11}{2}^-$  state was observed, it was expected to



TABLE I. Summary of numerical results of the Coriolis calculation of the negative-parity states in  $^{105}\text{Pd}$ . Energies are in keV. Nine states between 2886 and 4083 keV have been omitted for clarity (see Fig. 5). Contributions from the  $\frac{3}{2}^- [514]$  and the  $\frac{1}{2}^- [505]$  Nilsson states and  $R_0=10, 12$  were found near zero and omitted. Measured stripping and pick-up spectroscopic factors for the  $\frac{1}{2}^-$  state are given in parentheses.

I	Energy (Obs.)	Energy (Calc.)	Amount of Coriolis mixing $f_{JK}^2$			Calculated spect. factors $S_I(d,t)$	Calculated spect. factors $(2I+1)S_I(d,p)$	Fraction of R component $P(I_M, R_0)$					
			$\frac{1}{2}^- [550]$	$\frac{3}{2}^- [541]$	$\frac{5}{2}^- [532]$			$\frac{7}{2}^- [523]$	$R_0=0$	$R_0=2$	$R_0=4$	$R_0=6$	$R_0=8$
$\frac{1}{2}^-$	490	490	0.39	0.37	0.18	0.05	1.46(1.15)	6.28(6.05)	0.64	0.33	0.03	0.0	0.0
$\frac{1}{2}^-$	644	514	0.44	0.38	0.15	0.02			0.03	0.94	0.03	0.0	0.0
$\frac{3}{2}^-$	...	897	0.07	0.33	0.38	0.18			0.0	0.74	0.24	0.01	0.0
$\frac{5}{2}^-$	970	941	0.39	0.37	0.18	0.06			...	0.85	0.14	0.01	0.0
$\frac{7}{2}^-$	1087	1088	0.67	0.33	...	...			0.0	0.06	0.94	0.0	...
$\frac{9}{2}^-$	...	1188	0.16	0.54	0.31	...			0.0	0.04	0.93	0.04	0.0
$\frac{11}{2}^-$	...	1194	0.05	0.30	0.38	0.21			...	0.60	0.35	0.05	0.0
$\frac{13}{2}^-$	...	1584	0.20	0.01	0.15	0.36	0.03	2.65	0.21	0.23	0.49	0.07	0.00
$\frac{15}{2}^-$	...	1600	0.25	0.00	0.37	0.38			...	0.04	0.89	0.06	0.0
$\frac{17}{2}^-$	1742	1731	0.37	0.36	0.19	0.05			...	...	0.90	0.10	0.0
$\frac{19}{2}^-$	...	1911	0.12	0.23	0.00	0.34			0.0	0.23	0.49	0.27	0.01
$\frac{21}{2}^-$	...	1921	1.00	...	...	...			...	0.0	0.06	0.94	...
$\frac{23}{2}^-$	1961	1912	0.05	0.31	0.38	0.20			...	...	0.74	0.23	0.02
$\frac{25}{2}^-$	...	2256	0.33	0.67	...	...			...	0.0	0.05	0.95	0.0
$\frac{27}{2}^-$	...	2268	0.21	0.01	0.15	0.37			...	0.09	0.57	0.32	0.02
$\frac{29}{2}^-$	...	2276	0.34	0.07	0.59	...			...	0.0	0.08	0.87	0.05
$\frac{31}{2}^-$	...	2358	0.09	0.23	0.00	0.21			...	0.31	0.23	0.40	0.06
$\frac{33}{2}^-$	...	2514	0.13	0.01	0.22	0.01	0.04	1.23	0.11	0.34	0.15	0.38	0.03
$\frac{35}{2}^-$	...	2707	0.18	0.17	0.13	0.52			0.0	0.01	0.08	0.88	0.03
$\frac{37}{2}^-$	2700	2742	0.39	0.37	0.18	0.05			...	...	...	0.91	0.08
$\frac{39}{2}^-$	2901	2886	0.05	0.32	0.38	0.19			...	...	...	0.80	0.19
$\frac{41}{2}^-$	...	3327	0.50	0.39	0.10	...			...	...	0.0	0.11	0.89
$\frac{43}{2}^-$	3801	3975	0.40	0.37	0.18	0.05			...	...	...	...	0.92

contain nearly the full one-quasiparticle strength of  $(2I+1)S_I = 12.0U^2 \approx 12(U^2 \approx 1)$ . This discrepancy has been reported for heavier Pd nuclei.<sup>29</sup> The present Coriolis treatment places a significant fraction of the  $\frac{11}{2}^-$  strength at much higher energies, and tends to remove the discrepancy. The success of the calculation in predicting this spectroscopic factor is additional evidence for the validity of the model.

It is interesting to note that spectroscopic factors can be easily obtained from the  $R$  projections  $P(IM, R_0)$  [Eq. (9)]. Since the target is in an  $R=0$  state, single-nucleon transfer can only populate  $R=0$  components of final states. Thus, one finds<sup>27</sup> (for a pure single-particle state)

$$S_I = P(IM, R_0=0)U_I^2.$$

The tabulated  $P(IM, R_0=0)$  fractions of Table I therefore provide an alternate determination of single-nucleon-transfer spectroscopic factors.

The present simple Coriolis calculation has been successful in describing the  $\frac{11}{2}^-$ ,  $\Delta I=2$  band in the odd- $A$  Pd nuclei. The results of Fig. 5 clearly indicate why many other states (resulting from the coupling of the  $\frac{11}{2}^-$  state to the core excitations) were not observed in (HI,  $xn$ ) reactions; they are far from the yrast line. More importantly, the nature of the low-lying  $\frac{7}{2}^-$  and  $\frac{3}{2}^-$  states observed in  $\beta$  decay and some of the higher-lying high-spin states seen in the (HI,  $xn$ ) studies have been explained for the first time. The enhanced  $B(E2)$ 's for transitions between states in the rotation-aligned and rotation-antialigned bands have been adequately predicted, and the anomalous spectroscopic factor for the 490 keV  $\frac{11}{2}^-$  state has been explained. The overall success of the simple rotational treatment of the negative-parity states of these nuclei argues strongly for the validity of the approach and suggests that the more complex problem of the behavior of the positive-parity states of the odd- $A$  Pd nuclei might also be understood in the context of this simple model.

### B. Positive parity states

The experimental data on the positive-parity levels in  $^{101-105}\text{Pd}$  are much more abundant than for the negative-parity states, especially in  $^{103,105}\text{Pd}$ . In addition to the  $\frac{5}{2}^+$  and  $\frac{7}{2}^+$   $\Delta I=2$  bands seen in the (HI,  $xn$ ) work,<sup>1</sup> a number of lower-spin positive-parity states have been established through decay and reaction studies in  $^{103}\text{Pd}$  (see Ref. 25) and  $^{105}\text{Pd}$  (see Refs. 5 and 28).

In the negative-parity calculation,  $j$  was an extremely good quantum number, the  $C_{11/2}$  being larger than 0.96 for all six Nilsson states in the basis. In the positive-parity case, however, there

is a significant amount of  $j$  mixing in the basis states. To illustrate this we present in Table II the  $C_{j\kappa}^2$  for the positive-parity basis states. It is clear from this table that  $j$  is less prominent as a constant of the motion of the odd particle than in the negative-parity case. However, we see that it is clear which states are dominated by  $d_{5/2}$  and which states are largely  $g_{7/2}$  in character.

Because of the  $j$  mixing the first positive-parity calculations were carried out including in the basis all Nilsson states with  $g_{7/2}$ ,  $d_{5/2}$ ,  $d_{3/2}$ , and  $s_{1/2}$  parentage. The  $d_{3/2}$  and  $s_{1/2}$  Nilsson states were seen to play a minor role in the description of the (heavy ion,  $xn$ ) results. This was largely because their low  $j$  values resulted in small Coriolis matrix elements with the  $d_{5/2}$  and  $g_{7/2}$  states. Furthermore, their relatively high excitation energy (see Fig. 1), along with their small Coriolis matrix elements, resulted in only very small  $d_{3/2}$  and  $s_{1/2}$  admixtures in the other states in the calculation. Accordingly, as a simplification to the calculation, the  $d_{3/2}$  and  $s_{1/2}$  states were omitted from the set of positive-parity basis states.

The positive-parity calculation was performed with the moment of inertia parameters shown in Figs. 3(b) and 3(c). The only significant variation of the input parameters was that of the single-particle energy of the  $\frac{1}{2}[431]$  Nilsson state. In order to position the  $\frac{5}{2}^+$  state as the lowest energy state in each nucleus, it was necessary to raise the single-particle energy of this Nilsson state (see Fig. 1) by approximately 450 keV (thereby lowering the excitation energy).

The results of the calculation with the input described above are summarized in Figs. 6(a)–6(c) for  $A=101$ –105, respectively. As with the negative-parity calculation, the only changes made in going from  $A=101$  to  $A=105$  were in the specification of Fermi level (see Fig. 1) and mass number.

TABLE II. Spherical shell model state admixtures for the  $d_{5/2}$  and  $g_{7/2}$  Nilsson states, calculated with  $\delta=0.12$ ,  $\mu=0.35$ , and  $\kappa=0.0637$ . Also included are the  $\langle j^2 \rangle$  terms, as calculated from Eq. (4).

Nilsson State	$j = \frac{1}{2}$	$\frac{3}{2}$	$\frac{5}{2}$	$\frac{7}{2}$	$\frac{9}{2}$	$\langle j^2 \rangle$
$\frac{1}{2}[431]$	0.14	0.07	0.67	0.05	0.07	8.71
$\frac{2}{3}[422]$		0.05	0.73	0.17	0.05	10.37
$\frac{5}{2}[413]$			0.63	0.35	0.02	11.50
$\frac{1}{2}[420]$	0.00	0.14	0.11	0.74	0.00	13.31
$\frac{3}{2}[411]$		0.02	0.20	0.78	0.00	14.12
$\frac{5}{2}[402]$			0.35	0.65	0.00	13.29
$\frac{7}{2}[404]$				0.99	0.00	15.78

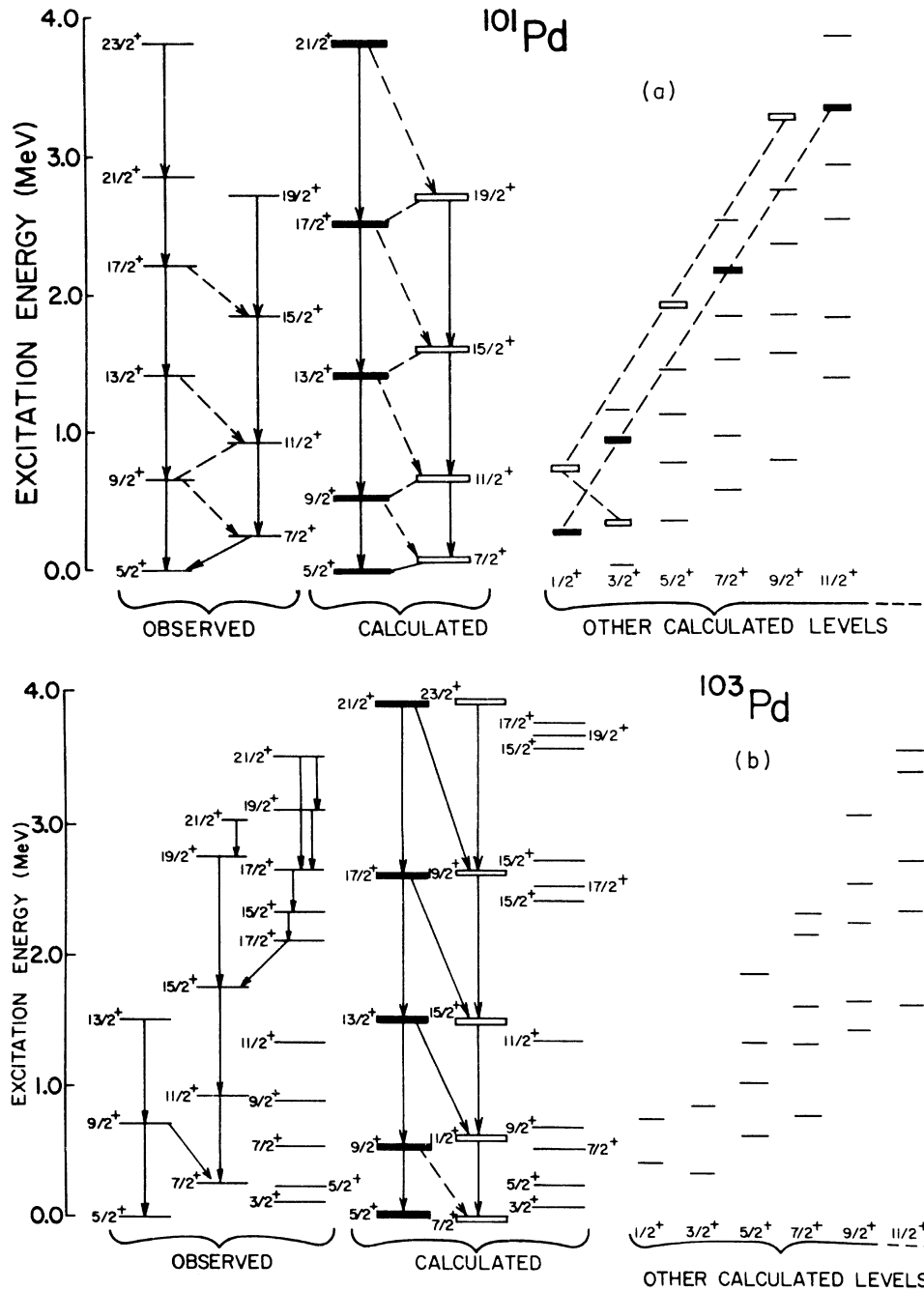


FIG. 6. (a) Summary of experimental and calculated results for the positive-parity levels in  $^{101}\text{Pd}$ . The arrows in the experimental spectrum denote observed transitions, with the solid lines indicating strong transitions and the dashed lines indicating weaker transitions. The corresponding arrows in the theoretical spectrum are meant to represent the fact that large  $E2$  matrix elements exist between states connected by solid arrows. Considerably weaker transitions are predicted between states connected by the dashed arrows. The states which are predicted to comprise the "rotation-antialigned" bands are highlighted among the other calculated levels, the solid lines representing the  $d_{5/2}$  band and the open lines denoting the  $g_{7/2}$  band. For further discussion of this level scheme, see text. (b) Same as (a), but for  $^{103}\text{Pd}$ . In this nucleus, the rotation-antialigned bands were not as evident in the calculation, and so no indication of their identity is made. (c) Same as (a), but for  $^{105}\text{Pd}$ . The states denoted as the  $5/2^+$  ground-state band were grouped as such because of the similarity in their wave functions (all of these states contained a large  $5/2^+[413]$  component).

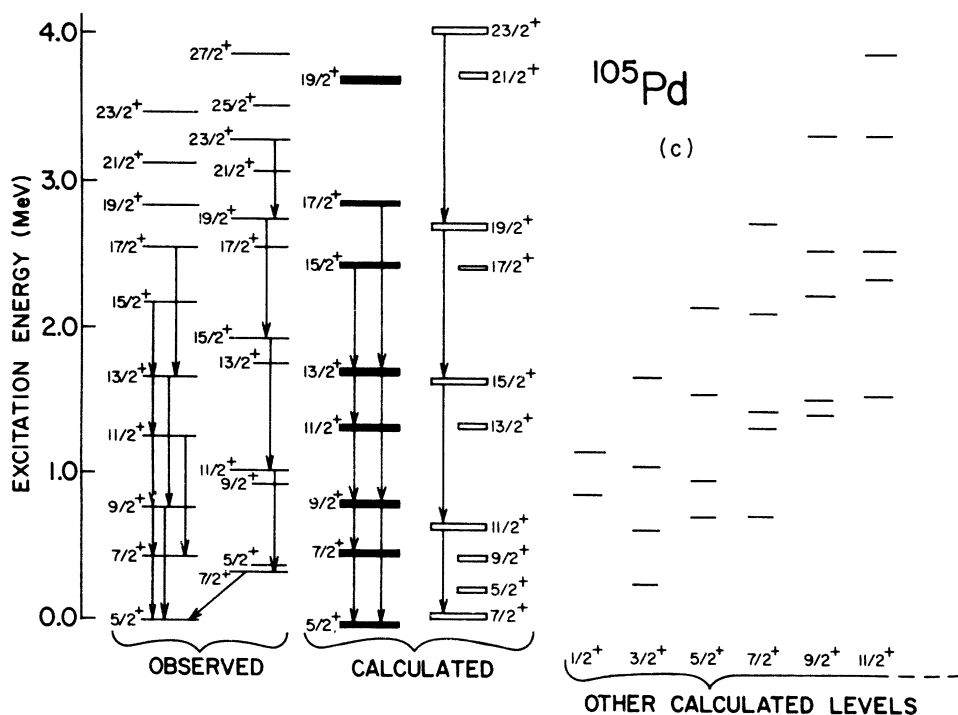


FIG. 6. (continued)

1.  $^{101}\text{Pd}$  levels

From Fig. 6(a) it is apparent that the present calculation reproduces the  $^{101}\text{Pd}$  level structure very well. Both a  $\frac{5}{2}^+$  and a  $\frac{7}{2}^+$   $\Delta I=2$  band of states are predicted theoretically. In addition, both bands exhibit the rotational composition [see Eq. (8)] expected for rotation-aligned bands (i.e., band-head largely  $R=0$ , first rotational state mostly  $R=2$ , etc.) The calculation further predicts that the states in each of the  $\frac{5}{2}^+$  and the  $\frac{7}{2}^+$   $\Delta I=2$  bands are linked by large  $E2$  intraband matrix elements, the  $B(E2\uparrow)$ 's being typically 20–30 single-particle units, while interband  $B(E2)$ 's are typically two orders of magnitude smaller. The weaker interband transition strength is carried by  $M1$  radiation.

The Coriolis-mixed wave functions of the  $\frac{7}{2}^+$  band of states show these states to be largely  $K=\frac{1}{2}$  in character, with some  $K=\frac{3}{2}$  admixed. The  $f_{IK}(\frac{1}{2}[420])$  is typically 0.66, while  $f_{IK}(\frac{3}{2}[411])$  is approximately 0.50. The  $\frac{5}{2}^+$  band is also calculated to be dominantly  $K=\frac{1}{2}$  and  $\frac{3}{2}$  in approximately equal amounts.  $\{f_{IK}(\frac{1}{2}[431])$  and  $f_{IK}(\frac{3}{2}[422])$  are typically 0.65 to 0.70.} These results, along with the rotational composition and  $B(E2)$  values, present the  $\frac{5}{2}^+$  and  $\frac{7}{2}^+$   $\Delta I=2$  bands in  $^{101}\text{Pd}$  as primarily rotation-aligned bands arising from the coupling of  $d_{5/2}$  and  $g_{7/2}$  odd-particle states to the rotating  $^{100}\text{Pd}$  core.

In addition to the  $\Delta I=2$  bands discussed above, the calculation also predicts the presence of a number of other low-spin positive-parity levels in the first MeV of excitation. The low-spin states which the calculation predicts to be the antialigned bands of  $g_{7/2}$  and  $d_{5/2}$  states are highlighted in Fig. 6(a), although none of these states were seen in the  $(\text{HI}, x\text{n}\gamma)$  studies.

2.  $^{103}\text{Pd}$  levels

Figure 6(b) summarizes the calculated and observed level spectra for  $^{103}\text{Pd}$ . In this nucleus four states in the  $\frac{7}{2}^+$   $\Delta I=2$  band and only three states in the  $\frac{5}{2}^+$   $\Delta I=2$  band are observed. In the calculation for the  $\frac{7}{2}^+$  band, the rotation-aligned character persists, in that (a)  $K=\frac{1}{2}$  and  $\frac{3}{2}$  amplitudes dominate the Coriolis-mixed wave functions, (b) the rotational composition of the members of the band is consistent with the rotation-aligned picture, and (c) the states in this band are linked by large  $B(E2)$  reduced matrix elements. In the  $\frac{5}{2}^+$  band, however, the rotation-aligned nature of the states is predicted to be weakening. While  $K=\frac{1}{2}$  character is still prevalent in the wave functions of the band members, the  $K=\frac{3}{2}$  and  $\frac{5}{2}$  amplitudes are dominant. The rotational ( $R$ ) composition of the states does survive, however, in the manner expected for a rotation-aligned band. Although

the favored states ( $\frac{5}{2}^+$ ,  $\frac{9}{2}^+$ , etc.) are still connected by enhanced  $B(E2)$ 's,  $\Delta I=1$  transitions are also predicted to be increasing in strength.

The experimental levels shown in Fig. 6(b) are taken largely from the (HI,  $xn$ ) work reported earlier.<sup>4</sup> Some of the low-lying low-spin levels shown have been taken from the compilation by Kocher.<sup>25</sup> In addition to the  $\Delta I=2$  bands, essentially all of the other observed states can be accounted for by the calculation. The most likely candidates for the observed  $\frac{3}{2}^+ - \frac{11}{2}^+$  sequence of states seen at low energy are grouped to the right of the other calculated levels. This band contains large amplitudes of  $\frac{3}{2}^+[422]$  and  $\frac{5}{2}^+[413]$  Nilsson states, and may represent the developing  $d_{5/2}$   $\Delta I=1$  band which appears in  $^{105}\text{Pd}$  (see below). There are also a number of higher-spin calculated levels which could be associated with the observed  $\frac{15}{2}^+$  to  $\frac{21}{2}^+$  levels that were not definitely connected with either of the  $\Delta I=2$  bands. Of those calculated higher-spin states shown in Fig. 6(b), some also show large  $\frac{3}{2}^+[411]$  and  $\frac{5}{2}^+[413]$  amplitudes and may therefore be continuations of the developing  $\Delta I=1$   $d_{5/2}$  band mentioned above.

### 3. $^{105}\text{Pd}$ levels

A comparison of the experimental and calculated results for  $^{105}\text{Pd}$  is presented in Fig. 6(c). The experimental spectrum [obtained largely from (HI,  $xn$ ) work<sup>5</sup> and also from various decay studies (see compilation by Bertrand<sup>26</sup>)] shows a persistent  $\frac{7}{2}^+$   $\Delta I=2$  band of states, but the  $\frac{5}{2}^+$  ground

state appears to have become the bandhead of a "normal"  $\Delta I=1$  band. The calculation is quite successful at predicting both of these effects. The  $\frac{7}{2}^+$  band is seen to be still rotation aligned, but this character is significantly weakened. The Coriolis-mixed wave functions of the members of this band are not as pronounced  $K=\frac{1}{2}$ , but  $K=\frac{3}{2}$  and  $K=\frac{5}{2}$  amplitudes are also present in comparable amounts. The incipience of a  $\Delta I=1$  character to this band is both evident experimentally and predicted theoretically. However, the  $E2$  crossover transitions still dominate the decay in this band, and so the  $\Delta I=2$  appearance weakly survives. The  $\frac{5}{2}^+$  band is predicted to be a conventional  $\Delta I=1$  band whose dominant Nilsson amplitude is that of the  $\frac{5}{2}^+[413]$  state. The calculation agrees very well with experimental results for this band until approximately spin  $\frac{15}{2}$  or  $\frac{17}{2}$ , where a dramatic back-bendinglike behavior ensues. Of course this simple Coriolis coupling calculation cannot reproduce such an effect.

### 4. General results

The present calculation predicts a definite trend in the behavior of all three nuclei under study here. In  $^{101}\text{Pd}$ , the  $K=\frac{1}{2}$  bands for both the  $d_{5/2}$  and the  $g_{7/2}$  states are very near the Fermi level, and so the "decoupling", or rotation alignment has the optimum opportunity to manifest itself. As the Fermi level rises, however, the calculation shows that the rotation-aligned character of both the  $d_{5/2}$  and the  $g_{7/2}$  bands diminishes, but the

TABLE III. Coriolis-mixed wave functions for the lowest  $\frac{5}{2}^+$ ,  $\frac{9}{2}^+$ , and  $\frac{7}{2}^+$ ,  $\frac{11}{2}^+$  pairs of states in  $^{101-105}\text{Pd}$ . In each case the amplitude  $f_{IK}$  (for  $I = \frac{5}{2}, \frac{9}{2}, \frac{7}{2}$ , or  $\frac{11}{2}$ ) is given [see Eq. (5)].

$K^+$	$I^+$	$d_{5/2}$			$I^+$	$g_{7/2}$		
		101	103	105		101	103	105
$\frac{1}{2}$ [431]	$\frac{5}{2}$	0.62	0.41	0.09	$\frac{7}{2}$	-0.30	-0.22	-0.12
	$\frac{9}{2}$	0.65	0.34	0.38	$\frac{11}{2}$	-0.27	-0.22	-0.14
$\frac{1}{2}$ [420]	$\frac{5}{2}$	0.12	0.01	-0.11	$\frac{7}{2}$	0.63	0.58	0.39
	$\frac{9}{2}$	0.13	-0.10	0.21	$\frac{11}{2}$	0.67	0.63	0.49
$\frac{3}{2}$ [422]	$\frac{5}{2}$	0.69	0.65	0.34	$\frac{7}{2}$	-0.43	-0.35	-0.24
	$\frac{9}{2}$	0.66	0.57	0.49	$\frac{11}{2}$	-0.35	-0.30	-0.23
$\frac{3}{2}$ [411]	$\frac{5}{2}$	0.03	-0.12	-0.35	$\frac{7}{2}$	0.45	0.53	0.54
	$\frac{9}{2}$	0.04	-0.34	0.37	$\frac{11}{2}$	0.49	0.55	0.59
$\frac{5}{2}$ [413]	$\frac{5}{2}$	0.35	0.63	0.82	$\frac{7}{2}$	-0.30	-0.36	-0.48
	$\frac{9}{2}$	0.34	0.58	0.55	$\frac{11}{2}$	-0.25	-0.28	-0.36
$\frac{5}{2}$ [402]	$\frac{5}{2}$	0.01	-0.05	-0.25	$\frac{7}{2}$	0.18	0.26	0.42
	$\frac{9}{2}$	-0.01	-0.25	0.36	$\frac{11}{2}$	0.21	0.27	0.41
$\frac{7}{2}$ [404]	$\frac{5}{2}$	...	...	...	$\frac{7}{2}$	0.09	0.14	0.29
	$\frac{9}{2}$	-0.06	-0.21	-0.02	$\frac{11}{2}$	0.09	0.12	0.23

$d_{5/2}$  band deteriorates much more rapidly. This is evidenced primarily by the change in the Coriolis mixing amplitudes in the wave functions for the states of these two bands. As an explicit example of this, we show in Table III the Coriolis-mixed wave functions for the  $\frac{5}{2}^+$  ground state and its  $\frac{9}{2}^+$  companion, as well as the lowest-lying  $\frac{7}{2}^+$  state and its  $\frac{11}{2}^+$  partner for  $^{101-105}\text{Pd}$ . Here we see explicitly the gradual loss of preference for alignment of  $\vec{j}$  and  $\vec{R}$  (ordinarily manifest by large  $K=\frac{1}{2}$  amplitudes) as mass increases.

With this "loss of alignment" should come a diminishing in the decoupled character of the bands. One way to witness this is to consider the  $B(E2)$  values for transitions in the  $\Delta I=2$  bands in comparison with corresponding  $E2$  transitions in the adjacent even-even cores. If the odd particle is minimally coupled to the core and the character of the excited states of the  $\Delta I=2$  bands is largely that of the rotating core, then the  $B(E2\uparrow)$  for transition from the  $R=2$  to the  $R=0$  states in these bands (i.e., the  $\frac{11}{2}^+ \rightarrow \frac{7}{2}^+$  and the  $\frac{9}{2}^+ \rightarrow \frac{5}{2}^+$  transitions in the  $\frac{7}{2}^+$  and  $\frac{5}{2}^+$  bands, respectively) would be equal to the  $B(E2, 2^+ \rightarrow 0^+)$  for the adjacent even-even core. The extent to which this is not true may be said to be a measure of the lack of decoupled rotation-aligned character in the band. Bolotin and McClure<sup>10</sup> quote values of  $B(E2, 2^+ \rightarrow 0^+)$  for  $^{110,108,106,104}\text{Pd}$  to be 0.172, 0.149, 0.131, and 0.106  $e^2b^2$ , respectively. This trend suggests that the corresponding values for  $^{102,100}\text{Pd}$  would likely be somewhat less than 0.100  $e^2b^2$ . The calculated values of the  $R=2$  to  $R=0$   $B(E2)$ 's in  $^{101-105}\text{Pd}$  are given in Table IV. In the context of the discussion above these results predict reasonably definite decoupling in  $^{101}\text{Pd}$ ,  $B(E2\uparrow)$  being nearly equal to the

expected  $B(E2, 2^+ \rightarrow 0^+)$  in  $^{100}\text{Pd}$ . However, the calculated values show a steady decrease with *increasing* mass, suggesting a gradual failure of the decoupled description for  $^{103}\text{Pd}$  and  $^{105}\text{Pd}$ . Furthermore, this failure is predicted to be much more rapid in the  $\frac{5}{2}^+$  band than in the  $\frac{7}{2}^+$  band, which is consistent with observation. It should also be noted that the  $B(E2\uparrow)$  measured by Bolotin and McClure<sup>10</sup> for the  $\frac{9}{2}^+ \rightarrow \frac{5}{2}^+$  ground-state transition in  $^{105}\text{Pd}$  is 0.035  $e^2b^2$ , which compares very well with our calculated value of 0.023  $e^2b^2$ . (The transition referred to here is the ground-state transition from the 782-keV state which the authors of Ref. 10 tentatively assumed to be  $\frac{7}{2}^+$ . In fact, the work of Ref. 5 establishes this state as the  $\frac{9}{2}^+$  member of the  $\frac{5}{2}^+$   $\Delta I=1$  band discussed above.) The work of these authors actually provided the earliest indication that the odd-mass Pd nuclei may be exhibiting some collective behavior. They observed several highly enhanced  $E2$  transitions in  $^{105}\text{Pd}$  and thereby suggested that the collective features of some of the  $^{105}\text{Pd}$  levels were important. These authors point out that in a weak-coupling core-excitation model,<sup>30,31</sup> transitions from each member of the  $d_{5/2}$  neutron- $2^+$  core phonon excitation multiplet would represent the  $2^+ \rightarrow 0^+$  core deexcitation, and the  $E2$  strength out of each of these multiplet members to the ground state should equal the  $B(E2, 2^+ \rightarrow 0^+)$  of the even-even core. They then show that significant  $B(E2\uparrow)$  strength in  $^{105}\text{Pd}$  exists only to the  $\frac{7}{2}^+$  and  $\frac{9}{2}^+$  states at 442 and 782 keV, respectively, and is otherwise severely fragmented among many other states. In addition, they show that a significant fraction of the expected  $E2$  strength from the ground state is missing from the Coulomb excitation spectrum. Their conclusion is that the core-excitation strength must be shared over many other low-lying levels in  $^{105}\text{Pd}$ , and the weak coupling description of this nucleus is unjustified. [In an earlier study of  $^{105}\text{Pd}$ , Krien, *et al.*<sup>32</sup> recognized this fact and attempted a Coriolis calculation on this nucleus—with mixed success, due to the fact that very little experimental data was available at the time.] Our calculation, on the other hand, is not predicated on any weak-coupling picture, but rather it relies upon the strong Coriolis coupling between the odd particle and the rotating, slightly deformed core. This model provides a natural mixing mechanism whereby the  $E2$  strength to the ground state is severely fragmented, and thus explains the observations in the Coulomb excitation studies.

As was indicated previously, the  $(d,p)$  and  $(d,t)$  spectroscopic factors have been measured<sup>28</sup> for the three Pd nuclei studied here. It is observed that in these nuclei the  $d_{5/2}$  and  $g_{7/2}$  single-particle strengths are concentrated largely in the ground

TABLE IV. Calculated  $B(E2\uparrow)$  values for the  $R=2$  to  $R=0$  transitions in the  $\frac{5}{2}^+$  and  $\frac{7}{2}^+$   $\Delta I=2$  bands in  $^{101-105}\text{Pd}$  (i.e., the  $\frac{9}{2}^+ \rightarrow \frac{5}{2}^+$  and  $\frac{11}{2}^+ \rightarrow \frac{7}{2}^+$  transitions in these nuclei).  $B(E2)$ 's are expressed in units of  $e^2b^2$ . Also given are the  $B(E2, 2^+ \rightarrow 0^+)$  in even-even Pd nuclei of mass number  $A=104$  to  $A=110$  (in the same units) from Ref. 10.

A	$B(E2\uparrow)$ ( $e^2b^2$ )	
	$\frac{9}{2}^+ \rightarrow \frac{5}{2}^+$	$\frac{11}{2}^+ \rightarrow \frac{7}{2}^+$
101	0.065	0.074
103	0.039	0.069
105	0.023	0.054
A	$B(E2, 2^+ \rightarrow 0^+)$ ( $e^2b^2$ )	
104	0.11	
106	0.13	
108	0.15	
110	0.17	

state and lowest-lying  $\frac{7}{2}^+$  state, respectively. However, the  $d_{5/2}$  single-particle strength in the odd-mass Pd ground state is observed to deteriorate dramatically from  $^{101}\text{Pd}$  to  $^{105}\text{Pd}$ . These results are summarized in Table V. Our calculations based on this simple rotational model are also summarized in Table V, and it is evident that the overall magnitudes of these spectroscopic factors are very well reproduced. It should be remarked that the predicted low-lying  $d_{5/2}$  strength seems to be concentrated slightly above the ground state in  $^{105}\text{Pd}$  and split between the two lowest-lying  $\frac{5}{2}^+$  states in  $^{103}\text{Pd}$  [see also Figs. 6(b) and 6(c)]. This probably suggests the need for a slight refinement of some of the input parameters for the calculations on these two nuclei, most likely the energies of the single-particle basis states (Fig. 1). We do not believe that any significant change in the major features of the theoretical predictions would result from such small adjustments of the input parameters so no such refinements were attempted, thereby preserving the simplicity of the calculation. In any case, the theoretical corroboration of the dramatic decrease in the  $d_{5/2}$  spectroscopic strength, accompanied by a general persistence of the  $g_{7/2}$  spectroscopic strength (and also of the  $h_{11/2}$  strength, which is included in Table V for completeness) as one goes from  $^{101}\text{Pd}$  to  $^{105}\text{Pd}$  is evident and therefore constitutes an additional success of this simple model.

#### IV. DISCUSSION

Some attempts have been made to describe the decoupled band structure in this mass region in terms of a model which utilizes a weak coupling of the odd particle to the phonon excitations of the even-even core. In this description the decoupled

$\Delta I=2$  bands arise from the weak coupling of the appropriate odd particle to the aligned multiple phonon states of the core. The fact that both this model and the rotational model exhibit similar success in reproducing the energies of the decoupled bands is easy to understand. The aligned members of the multiple phonon excitations ( $I^\pi = 2n^+$  for the  $n$ -phonon multiplet) viewed microscopically, involve coherent nucleon motion not unlike that arising from the rotational motion of an ellipsoidal core. However, the success of the weak-coupling particle-phonon model is limited to the  $\Delta I=2$  bands; it is not at all successful in explaining the other "unfavored" states observed experimentally in  $^{103,105}\text{Pd}$ . The ease with which the rotational model explains these additional states is therefore compelling evidence for its validity in these nuclei.

Central to the success of the present calculation has been the treatment of the moment of inertia parameters for these odd-mass Pd nuclei. It is essential that these parameters decrease (i.e., the nuclear moment of inertia increase) with increasing nuclear spin in order to reproduce the observed compression of the  $\Delta I=2$  bands. There is an added provision that the  $K=\frac{1}{2}$  bands possess an oscillating moment of inertia parameter, reflecting the fact that the dominant character of the states in these bands alternates between an aligned and a nonaligned configuration, the alignment being that of the  $\vec{j}$  of the odd particle and the  $\vec{R}$  of the even-even core. The simplified extension of the VMI procedure which we have adopted [see Eqs. (16), (18), and (19)] accomplishes this task to a reasonable first approximation. The *wave functions* are still constructed under the assumption of a constant deformation  $\delta (=0.12)$ . Thus, the intrinsic Coriolis matrix elements, as well as reduced electromag-

TABLE V. Comparison of theoretical single-nucleon-transfer spectroscopic factors with their measured values (from Ref. 28). For definitions of the spectroscopic factors, see Eqs. (10) and (11).

Isotope of Pd	$I^\pi$	$(2I+1)S(d,p)$		$S(d,t)$	
		Observed	Calculated	Observed	Calculated
101	$\frac{5}{2}^+$	(3.99) <sup>a</sup>	3.30	(1.71)	1.97
103		3.00	1.63/0.80 <sup>b</sup>	1.82	1.85/0.86
105		1.24	0.34/1.74	1.10	0.55/1.74
101	$\frac{7}{2}^+$	(4.08)	4.48	(2.72)	1.41
103		3.79	3.94	2.53	2.08
105		5.22	3.72	3.34	2.66
101	$\frac{11}{2}^-$	(7.02)	6.98	(0.78)	0.54
103		6.58	6.72	0.98	0.84
105		6.05	6.28	1.15	1.44

<sup>a</sup> Extrapolated values from Ref. 28 given in parentheses.

<sup>b</sup> Two  $\frac{5}{2}^+$  states of significant strength were calculated in  $^{103,105}\text{Pd}$ . Spectroscopic factors for these states are given as follows: lowest-energy  $\frac{5}{2}^+$ /second-lowest  $\frac{5}{2}^+$ .

netic transition matrix elements, do not fully reflect the dynamic behavior of  $\delta$ . Actually, in the unique-parity ( $h_{11/2}$ ) case, it should be no surprise that this approximation does not diminish the success of the calculation. The  $C_{jK}$  ( $j = \frac{11}{2}$ ) is  $\approx 1.0$  over a very wide range of values for  $\delta$ , and so the Nilsson wave functions are negligibly perturbed by the changing  $\delta$ . In the positive-parity case, however, the configuration mixing is much more sensitive to  $\delta$ , and so refinements in the treatment of the variations in  $\delta$  should improve the calculation.

It is likely that the parameters  $C$  and  $g_{0K}$ , as used in this calculation, cannot properly be assigned the physical significance of an elastic constant and a minimum moment of inertia as they are in the even-even case. In a completely self-consistent treatment, such an association would still seem reasonable; but in the present calculation these two quantities are viewed simply as parameters which help us compensate in part for some of the inconsistencies of the simplified approach.

In spite of the dramatic rate of change of the moments of inertia of these light Pd nuclei with angular momentum, it is not really proper to view these nuclei as particularly "soft" toward deformation. Indeed, VMI fits to the even-even Pd nuclei in this region<sup>15</sup> yield an elastic constant  $C$  on the order of  $6 \times 10^6 \text{ keV}^3$ , which is in accord with values typical for rare-earth nuclei ( $\sim 2$  to  $10 \times 10^6 \text{ keV}^3$ ).<sup>16</sup> The Pd nuclei are unique in that their small moments of inertia require very large rotational frequencies for even a modest amount of angular momentum. For instance, a simple calculation reveals that the rotational frequency associated with the  $2^+$  state in  $^{102}\text{Pd}$  is about the same as that of a  $10^+$  or  $12^+$  state in a rare-earth nucleus. Thus, it is easy to see why Coriolis effects (the classical force being proportional to  $|\vec{\omega}_{\text{core}} \times \vec{j}_{\text{particle}}|$ ) are so strong in these intermediately deformed nuclei. Furthermore, at these high rotational frequencies, one must also be aware of other shape degrees of freedom in the nuclear dynamics. In particular, nonaxially-symmetric shapes may become important as the nuclear spin increases. The triaxial-rotor-plus particle model of J. Meyer-Ter-Vehn<sup>37</sup> has had some measure of success in explaining the data for the  $A \approx 135$  and  $A \approx 190$  transitional regions,<sup>38</sup> and Toki and Faessler<sup>39</sup> have attempted a similar approach in the  $A \approx 100$  region. However, the present calculations would suggest that in order to reproduce the data properly, it will be necessary to treat the  $\beta$  and probably also the  $\gamma$  degrees of freedom as dynamic variables.

Another important aspect of the present calculation is the inclusion of the so-called "recoil term" in the expression of the rotational energy.<sup>13,40</sup> The

primary component of this term is the  $(\langle j^2 \rangle - K^2)$  portion of the rotational energy [see Eq. (16)]. For the  $\Delta I = 2$  bands considered here, the main contribution to the rotational energy comes from the  $\langle j^2 \rangle$  term (since  $K \approx \frac{1}{2}$ ), which can be quite large. The essential effect of this term is a constant addition to the "zero-point energy", and is properly added to the *quasiparticle* band-member energies.<sup>40</sup> For a typical moment of inertia parameter of 60 keV (see Fig. 3 and Table II), this results in an upward displacement of the  $d_{5/2}$  bands by  $\approx 600$  keV, the  $g_{7/2}$  bands by  $\approx 850$  keV, and the  $h_{11/2}$  bands by  $\approx 2.5$  MeV. This latter result for the  $h_{11/2}$  bands is essential to the mutual consistency of the energetics of the positive- and negative-parity calculations. As was mentioned in Sec. II, the  $h_{11/2}$  states were positioned relative to the  $N = 4$  Nilsson states so that the  $h_{11/2}$  energy at  $\delta = 0$  was consistent with the value deduced by the fits of Reehal and Sorensen<sup>8</sup> to the energies and  $B(E2)$  values out of the levels of single-particle shell model nuclei in this mass region (see Fig. 1). In some calculations in this mass region (see, e.g., Ref. 41) it was necessary to place the  $h_{11/2}$  state  $\sim 1$  MeV above all of the  $N = 4$  Nilsson states, which was not consistent with shell-model results.<sup>8</sup> On the other hand, placement of the  $h_{11/2}$  as shown in Fig. 1 yields consistent results, the necessary extra excitation of the  $h_{11/2}$  bands being provided by the  $\langle j^2 \rangle$  term.

## V. CONCLUSIONS

It is our conclusion that the present work demonstrates that the level spectra of the odd- $A$  Pd nuclei in this mass region are best described by a rotational model with Coriolis coupling at intermediate deformation. It is encouraging that such a simplified application of the model yields results which correspond so well with the variety of experimental data discussed here. On the other hand, one can readily visualize improvements to the model which will help to resolve some of the minor discrepancies between the present results and the experimental data. The most important next step in improving the model would be a rigorously self-consistent treatment of the effective moment of inertia in this mass region where deformation seems to be an additional dynamic variable. It is anticipated that this work will provide some guidance for future efforts to refine the theoretical treatment of this problem and to improve the theoretical model for these quasirotational nuclei.

## ACKNOWLEDGMENTS

The authors wish to thank Professor G. T. Emery, Professor P. P. Singh, Professor F. B. Mal-



ik, Professor S. M. Harris, Professor F. S. Stephens, and Dr. T. E. Ward for some very helpful discussions. We are indebted to Dr. L. E. Samuelson and Dr. J. A. Grau for their assistance in per-

forming calculations. A brief but enlightening discussion with Professor Aage Bohr is also gratefully acknowledged.

\*Work supported in part by the National Science Foundation.

- <sup>1</sup>F. A. Rickey and P. C. Simms, *Phys. Rev. Lett.* **31**, 404 (1973).
- <sup>2</sup>F. S. Stephens, R. M. Diamond, J. R. Leigh, T. Kam-muri, and K. Nakai, *Phys. Rev. Lett.* **29**, 438 (1972).
- <sup>3</sup>P. C. Simms, G. J. Smith, F. A. Rickey, J. A. Grau, J. R. Tesmer and R. M. Steffen, *Phys. Rev. C* **9**, 684 (1974).
- <sup>4</sup>J. A. Grau, F. A. Rickey, G. J. Smith, P. C. Simms, and J. R. Tesmer, *Nucl. Phys.* **A229**, 346 (1974).
- <sup>5</sup>F. A. Rickey, J. A. Grau, L. E. Samuelson, and P. C. Simms (unpublished).
- <sup>6</sup>J. W. Starnier and M. E. Bunker (private communication).
- <sup>7</sup>S. G. Nilsson, *K. Dan. Vidensk. Selsk. Mat.-Fys. Medd.* **29**, No. 16 (1955).
- <sup>8</sup>B. Reehal and R. Sorensen, *Phys. Rev. C* **2**, 819 (1970).
- <sup>9</sup>V. G. Soloviev, *Theory of Complex Nuclei* (Moscow, 1971), p. 62.
- <sup>10</sup>H. H. Bolotin and D. A. McClure, *Phys. Rev. C* **3**, 797 (1971).
- <sup>11</sup>A. Bohr and B. Mottleson, *Nuclear Structure* (Benjamin, New York, 1969), Vol. 1, p. 169.
- <sup>12</sup>W. Ogle *et al.*, *Rev. Mod. Phys.* **43**, 424 (1971).
- <sup>13</sup>B. S. Nielsen and M. E. Bunker, *Nucl. Phys.* **A245**, 376 (1975).
- <sup>14</sup>P. Vogel, *Phys. Lett.* **33B**, 400 (1970).
- <sup>15</sup>P. C. Simms *et al.*, *Phys. Rev. C* **7**, 1631 (1973).
- <sup>16</sup>M. A. J. Mariscotti, G. Scharff-Goldhaber, and B. Buck, *Phys. Rev.* **178**, 1864 (1969).
- <sup>17</sup>A. B. Volkov, *Phys. Lett.* **41B**, 1 (1972).
- <sup>18</sup>P. R. Gregory and T. Taylor, *Phys. Lett.* **41B**, 122 (1972).
- <sup>19</sup>S. A. Hjorth, A. Johnson, and G. Ehrling, *Nucl. Phys.* **A181**, 113 (1972).
- <sup>20</sup>M. E. Bunker and C. W. Reich, *Rev. Mod. Phys.* **43**, 348 (1971); **44**, 126(E) 1972).
- <sup>21</sup>W. Scholz and F. B. Malik, *Phys. Rev.* **176**, 1355 (1968).
- <sup>22</sup>H. Kawakami and K. Hisatake, *Nucl. Phys.* **A149**, 523 (1970).
- <sup>23</sup>M. Berhar and Z. W. Grabowski, *Nucl. Phys.* **A196**, 412 (1972).
- <sup>24</sup>B. Nyman *et al.* (private communication to author of Ref. 25).
- <sup>25</sup>D. C. Kocher, *Nucl. Data Sheets* **13**, 337 (1974).
- <sup>26</sup>F. E. Bertrand, *Nucl. Data Sheets* **11**, 470 (1974).
- <sup>27</sup>G. R. Satchler, *Ann. Phys. (N.Y.)* **3**, 275 (1958).
- <sup>28</sup>F. A. Rickey, R. E. Anderson, and J. R. Tesmer (unpublished).
- <sup>29</sup>B. L. Cohen, R. A. Moyer, J. B. Moorhead, L. H. Goldman, and R. C. Diehl, *Phys. Rev.* **176**, 1401 (1968).
- <sup>30</sup>R. D. Lawson and J. L. Uretsky, *Phys. Rev.* **108**, 1300 (1957).
- <sup>31</sup>A. de-Shalit, *Phys. Rev.* **122**, 1530 (1960).
- <sup>32</sup>K. Krien, E. Spejewski, R. A. Naumann, and H. Hübel, *Phys. Rev. C* **6**, 1847 (1972).
- <sup>33</sup>H. J. Wiebicke and L. Münchow, *Phys. Lett.* **50B**, 429 (1974).
- <sup>34</sup>O. Häusser *et al.*, *Phys. Lett.* **52B**, 329 (1974).
- <sup>35</sup>Y. Tanaka and R. K. Sheline, *Phys. Lett.* **58B**, 414 (1975).
- <sup>36</sup>U. Hagemann and F. Döna, *Phys. Lett.* **59B**, 321 (1975).
- <sup>37</sup>J. Meyer-Ter-Vehn, *Nucl. Phys.* **A249**, 111 (1975).
- <sup>38</sup>J. Meyer-Ter-Vehn, *Nucl. Phys.* **A249**, 149 (1975).
- <sup>39</sup>H. Toki and A. Faessler, *Nucl. Phys.* **A253**, 231 (1975).
- <sup>40</sup>E. Osnes, J. Rekstad, and O. K. Gjotterud, *Nucl. Phys.* **A253**, 231 (1975).
- <sup>41</sup>A. Faessler, J. E. Galonska, U. Gotz, and H. C. Pauli, *Nucl. Phys.* **A230**, 302 (1974).